Journal of Statistical Physics, Vol. 64, Nos. 3/4, 1991

Kinetic Six-Vertex Model as Model of bcc Crystal Growth

M. Kotrla[1,2] and A. C. Levi[1]

Received November 15, 1990

The growth of bcc crystals is studied using van Beijeren's mapping onto the six-vertex model. The growth-evaporation processes are described in terms of vertices. The time evolution is given by a master equation for the probability of the six-vertex configurations. The model, studied in the finite-size case by both Monte Carlo and analytic methods, applies to the (001) surface and its vicinal surfaces. Different growth modes (including nucleation) are found, depending on the strength of disequilibrium and on temperature, and the transition between them is investigated.

KEY WORDS: Growth; nucleation; roughness; six-vertex model; stochastic.

1. INTRODUCTION

The problem of crystal growth has been theoretically studied for a long time and from different points of view. Already at an early stage it was found that there are two different modes of growth: layer-by-layer (Frank–van der Merwe) and continuous (Volmer–Weber) growth. It was pointed out that they are connected with the (smooth or rough) structure of the surface.[1] The roughening transition is reasonably well understood in equilibrium[2,3]; however, its nature in systems which are far from equilibrium is not.

It has emerged from the numerical simulations of simple ballistic models of crystal growth that the width of the surface obeys a nontrivial scaling law with increasing time or system size.[4] This opens the way to the possibility of classifying the growth models, in analogy with the critical

[1] SISSA, Miramare, 34014 Trieste, Italy.

[2] On leave of absence from the Institute of Physics, Czechoslovak Academy of Science, Prague, Czechoslovakia.

0022-4715/91/0800-0579$06.50/0

phenomena, into universality classes. Kardar *et al.*[5] carried out the renormalization group study of a nonlinear Langevin equation proposed to govern these universality classes. They predict a kinetic roughening transition for space dimensions $d > d_c = 2 + 1$. On the other side, Chui and Weeks[6] and later Nozières and Gallet[7] studied the linear response of a crystalline interface to a driving force. In the range of small driving forces they found a transition between two modes of growth. This kinetic roughening transition has been recently reexamined by Hwa *et al.*[8] Kertész and Wolf investigated the morphology of a model related to directed percolation and they obtained a different kind of kinetic roughening transition existing also in two dimensions.[9] Very recently several numerical simulations have been carried out indicating a transition also in other models.[10–14] However, the relation between the kinetic roughening transition and the transition between different growth modes far from equilibrium, if any, is still not clear.

Recently Garrod *et al.*[15] developed a stochastic three-dimensional model of crystal growth applicable to a simple cubic crystal and showed that it can be mapped onto a five-vertex model. They obtained exact results for the growth rate in the case of a finite-size system. Furthermore, using this mapping and the exact solution of the five-vertex model,[16] some exact statements could be derived in the case of the thermodynamic limit.[17] In the particular case of the (111) surface this model appears to be equivalent to the hypercube stacking model of Forrest and Tang[18] in $2 + 1$ dimensions. It has been proven[13] that the latter model has a kinetic roughening transition[9] in $3 + 1$ dimensions; the situation in $2 + 1$ dimensions is not yet quite clear.

The model of Garrod *et al.* has, however, the defect that it predicts a zero growth rate for the surfaces with one or two Miller indices equal to zero. This unrealistic effect is due to the use of a simplified picture, where only the so-called kink condensation and evaporation processes are considered, while the other processes important for the growth of surfaces lying near to the principal planes are not included. Moreover, to obtain a physical picture of the possible transition between growth modes, a relatively complex model where different growth modes occur must be considered. Such a more realistic model should contain at least two parameters: temperature and disequilibrium.

In this paper we address the problem of generalizing the work of Garrod *et al.* to the surfaces close to the principal planes, including the temperature dependence. In two dimensions simple models of this type have been studied, and exactly solved, by Gates and Westcott[19] and Garrod.[20] A three-dimensional model of crystal growth, where the surface lies near the principal plane, should allow a description of two-dimensional

nucleation. This problem has been already studied in the past in the case of simple cubic (sc) crystals using different approximations: classical Becker–Döring theory[21] or an approximative solution of kinetic equations.[3]

In the case of the solid-on-solid (SOS) model for a simple cubic crystal the mapping analogous to Garrod *et al.*'s leads to a rather complicated model which would contain at least 19 different vertices, because even if the level difference of nearest neighbors (n.n.) is restricted to be only zero or one (restricted solid-on-solid model), there are still 19 different configurations for the atomic levels on the plaquette of four neighboring sites (compare ref. 22). The situation is simpler in the case of a bcc crystal. One can use the mapping of the surface of a body-centered solid-on-solid (BCSOS) model onto the six-vertex model, proposed by van Beijeren[23] in connection with the thermal equilibrium roughening transition. The six-vertex model is the two-dimensional version of the *ice model*, introduced by Pauling and Slater[24] in order to study the residual entropy of ice at $T=0$ as well as the ferroelectric phase transitions. It is exactly solvable[25,26] and the BCSOS model is mapped into its particular case, the so-called F-model, which has a phase transition of infinite order. Hence van Beijeren's mapping allows an exact description of thermal roughening in the BCSOS model. We use this mapping for the study of a nonequilibrium phenomenon: the growth of bcc crystals. This leads to the problem of solving a kinetic (i.e., time dependent) six-vertex model. A special case of the model presented here was considered, among many other models, by Meakin *et al.*[27]

In Section 2 the model is formulated. In Section 3 the master equation is given and exact solutions for small size are presented, in Section 4 the simulation of the growth-evaporation process is described, and in Section 5 its results are given and discussed.

2. DESCRIPTION OF THE MODEL

We assume that condensation and evaporation are single-atom Markov processes and that the events on different sites are statistically independent. There are different kinds of these processes with different probabilities according to the surroundings of the site where they take place. We describe the situation first in the case of the sc lattice, in which the different possibilities are easily visualized. The typical processes on the surface of a sc crystal fulfilling the SOS condition are shown in Fig. 1. We shall call them, for later purposes, hill (Fig. 1a), cape (Fig. 1b), kink (Fig. 1c), ridge (Fig. 1d), valley (Fig. 1e), gulf (Fig. 1f), and lake (Fig. 1g) processes. Let us note that they correspond to the change of 1, 2, 3, 3, 3,

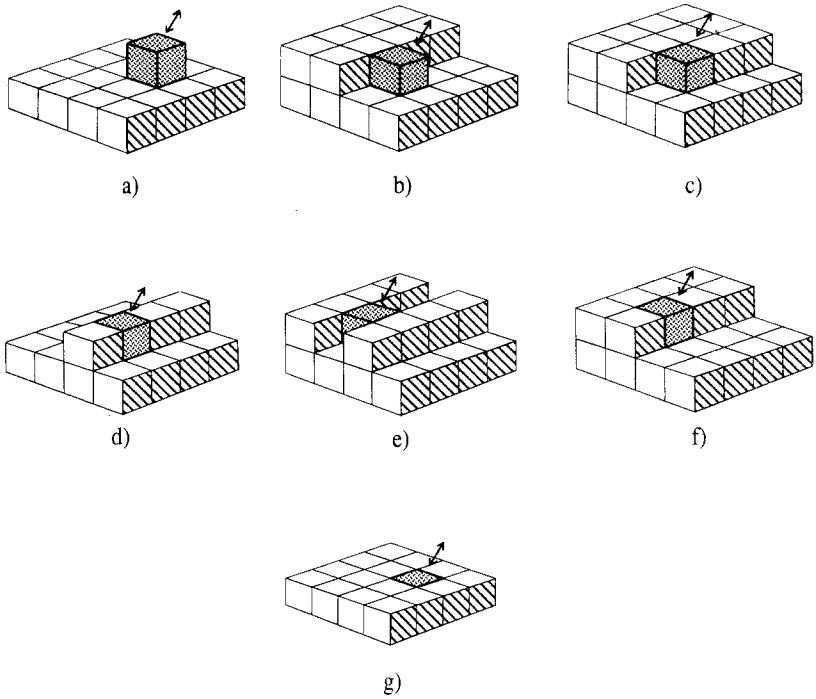

Fig. 1. The different kinds of growth-evaporation process on the surface of a simple cubic lattice.

4, and 5 bonds to n.n. Other configurations for the given kind of process can be generated by rotating by a multiple of $\pi/2$.

To get a tractable model, some assumption has to be made about the possible processes and their probabilities. In the model of Garrod *et al.*[15] only one process (kink from Fig. 1c) was allowed. In the case of a surface lying near the principal plane we are forced to consider all processes shown in Fig. 1, including all possibilities obtained by rotation. In particular, we have four kink processes instead of only one in the model of Garrod *et al.* For sake of simplicity the probability of a process may be assumed to depend only on the change of the number of bonds to n.n. atoms. Then there are 16 possible processes separated into five groups according to the number of bonds formed or broken. In the case of a bcc lattice (van Beijeren's model), which we are going to study, the same processes can be considered. The only difference is that instead of the bonds to n.n. (whose number now does not change) we have to consider the bonds to next nearest neighbors (n.n.n.): i.e., the sc crystal corresponds to a sublattice of the bcc crystal.

To fix ideas let us consider the bcc crystal with lattice spacing a, separated into two sublattices: (A) atoms at the corners and (B) atoms at the center. To describe the surface in the z direction we consider the square lattice with the spacing $a/\sqrt{2}$ rotated by $\pi/4$ with respect to the x, y axes of the bcc crystal (Fig. 2a). The height h_j of the surface in the z direction is measured using $a/2$ as a unit (Fig. 2b); here j labels the sites on the square lattice. Two neighboring sites i, j on this lattice correspond to the projection of atoms from different sublattices of the bcc lattice, so the difference $h_i - h_j$ has to be nonzero. In van Beijeren's model[23] this difference can have only two values $\pm a/2$. Then there are only six possible level configurations for the closed loop of four neighboring sites. If arrows are drawn across the bonds between the neighboring sites leaving the higher level atom on the right of the arrow, then a one-to-one correspondence between the surface in van Beijeren's model and the configurations of the six-vertex model[25] is obtained. An example of this correspondence is given in Figs. 2c and 2d. The six vertices are shown in Fig. 3 using arrows and also the so-called *line representation* in which segments occupied by arrows pointing down or to the left are marked by a solid line while segments occupied by arrows pointing up or to the right are left blank.

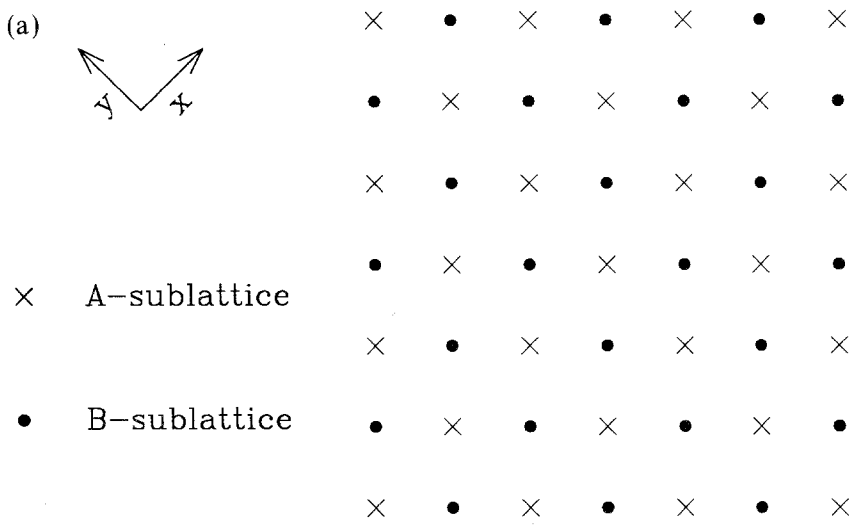

Fig. 2. (a) The square lattice corresponding to the projection of the two sublattices of the bcc lattice; x and y are orientations of the bcc lattice. (b) An example of the field of heights for the (013) surface. (c) The configuration of arrows corresponding to the levels in part (b). (d) The same configuration described in terms of vertices. (e) The terrace-ledge-kink structure for the surface from part (b). The numbers label different levels.

(b)

0	1	0	1	2	1	2
1	0	1	2	1	2	3
0	1	2	3	2	3	2
1	2	1	2	3	2	3
2	1	2	3	2	3	4
1	2	3	2	3	4	3
2	3	2	3	4	3	4

(c)

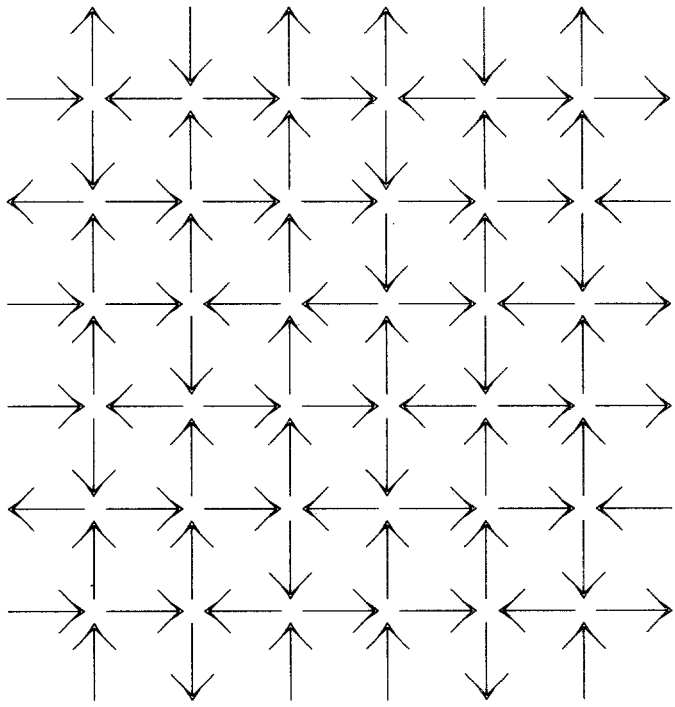

Fig. 2. (*Continued*)

(d)

5 6 1 5 6 1

6 1 1 3 1 5

1 5 4 6 5 6

5 6 1 5 6 1

6 1 5 6 1 5

1 5 6 1 5 6

(e)

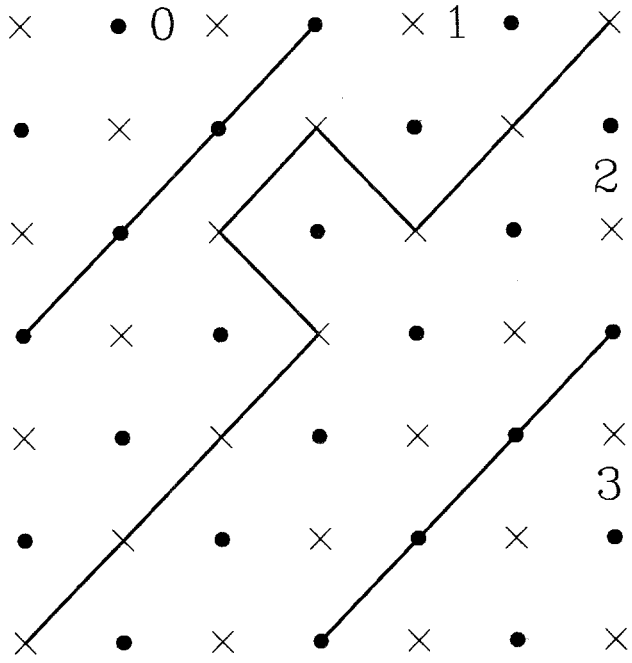

Fig. 2. (*Continued*)

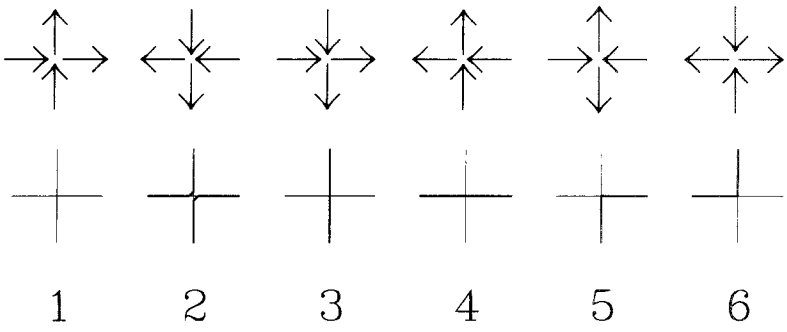

Fig. 3. The six vertices and their line representation.

Due to the alternation of the sublattices there is no sharp step structure separating layers on the bcc surface; one can, however, represent the decrease or increase of the levels and so visualize the growth-evaporation processes using the following rule. Let us consider a segment connecting two n.n. sites in one sublattice (i.e., two n.n.n.). There are two sites from the opposite sublattice adjoint to it. Mark the segment with a solid line if the levels of the adjoint sites are different and leave it blank otherwise. An example of this picture is in Fig. 2e. This line picture is different from the line representation of the six-vertex model. It affords a visualization of islands relevant for 2D nucleation, but has the drawback that it does not allow us to distinguish between the two "flat" configurations: (i) $h_A = na$, $h_B = (n+1/2)a$ and (ii) $h_A = na$, $h_B = (n-1/2)a$, which, in the six-vertex description, correspond to two different vertex configurations.

A growth-evaporation process at site j means the change of h_j by $\pm a$. Due to the constraint on the level difference of n.n. atoms this change is possible only on some sites. Let us call $\{v\} = \{v_i\}$ the possible configuration of the six-vertex model, where v_i is the vertex on the site i of the lattice dual to our initial square lattice. Then the growth-evaporation process is described in terms of vertices as a change $V_i \to \tilde{V}_i$ of a plaquette of the four neighboring vertices

$$V_i = \begin{pmatrix} v_{i+v} & v_{i+v+h} \\ v_i & v_{i+h} \end{pmatrix} \tag{1}$$

Here h and v stand for unit shifts parallel to the axes of the square lattice. The 16 possible processes in our model (labeled by $a = 1,\ldots, 16$) are explicitly listed below:

Hill, $a = 1$

$$\begin{pmatrix} 56 \\ 65 \end{pmatrix} \leftrightarrow \begin{pmatrix} 13 \\ 42 \end{pmatrix} \tag{2}$$

Cape, $a = 2, 3, 4, 5$

$$\begin{pmatrix}56\\61\end{pmatrix} \leftrightarrow \begin{pmatrix}13\\46\end{pmatrix}, \quad \begin{pmatrix}54\\65\end{pmatrix} \leftrightarrow \begin{pmatrix}15\\42\end{pmatrix}, \quad \begin{pmatrix}26\\65\end{pmatrix} \leftrightarrow \begin{pmatrix}63\\42\end{pmatrix}, \quad \begin{pmatrix}56\\35\end{pmatrix} \leftrightarrow \begin{pmatrix}13\\52\end{pmatrix} \tag{3}$$

Kink, $a = 6, 7, 8, 9$

$$\begin{pmatrix}56\\31\end{pmatrix} \leftrightarrow \begin{pmatrix}13\\56\end{pmatrix}, \quad \begin{pmatrix}54\\61\end{pmatrix} \leftrightarrow \begin{pmatrix}15\\46\end{pmatrix}, \quad \begin{pmatrix}24\\65\end{pmatrix} \leftrightarrow \begin{pmatrix}65\\42\end{pmatrix}, \quad \begin{pmatrix}26\\35\end{pmatrix} \leftrightarrow \begin{pmatrix}63\\52\end{pmatrix} \tag{4}$$

Ridge and valley, $a = 10, 11$

$$\begin{pmatrix}54\\35\end{pmatrix} \leftrightarrow \begin{pmatrix}15\\52\end{pmatrix}, \quad \begin{pmatrix}26\\61\end{pmatrix} \leftrightarrow \begin{pmatrix}63\\46\end{pmatrix} \tag{5}$$

Gulf, $a = 12, 13, 14, 15$

$$\begin{pmatrix}54\\31\end{pmatrix} \leftrightarrow \begin{pmatrix}15\\56\end{pmatrix}, \quad \begin{pmatrix}24\\61\end{pmatrix} \leftrightarrow \begin{pmatrix}65\\46\end{pmatrix}, \quad \begin{pmatrix}24\\35\end{pmatrix} \leftrightarrow \begin{pmatrix}65\\52\end{pmatrix}, \quad \begin{pmatrix}26\\31\end{pmatrix} \leftrightarrow \begin{pmatrix}63\\56\end{pmatrix} \tag{6}$$

Lake, $a = 16$

$$\begin{pmatrix}24\\31\end{pmatrix} \leftrightarrow \begin{pmatrix}65\\56\end{pmatrix} \tag{7}$$

The transitions from left to right correspond to condensation with "probability" C^a and the reverse transitions to evaporation with "probability" E^a. We write "probability" in quotes because the quantities considered may be just proportional, rather than equal, to probabilities (see below).

The "probabilities" C^a and E^a depend on the type a of process, i.e., on the geometry of the surroundings, and on the strength of the dis-equilibrium. We assume C^a and E^a to be determined by the change of the number of bonds to n.n.n. (n.n. in the sublattice). This can be expressed as a dependence on the change of the energy of the six-vertex model $E_v = \sum_i \varepsilon_{v_i}$ with vertex energies $\varepsilon_1 = \varepsilon_2 = \varepsilon_3 = \varepsilon_4 = \varepsilon$, $\varepsilon_5 = \varepsilon_6 = 0$. The effect of

the disequilibrium should be contained only in the "probabilities" for condensation. For a process $V_i \to \tilde{V}_i$ the Glauber kinetics[28] will be used in the following form:

$$C(V_i \to \tilde{V}_i) = \frac{e^{\beta \Delta\mu}}{e^{\beta \Delta E} + 1} \qquad \text{for condensation}$$
$$E(V_i \to \tilde{V}_i) = \frac{1}{e^{\beta \Delta E} + 1} \qquad \text{for evaporation} \tag{8}$$

where $\Delta E = E_{\tilde{V}} - E_V$ and $\beta = 1/(k_B T)$ gives the temperature. Since for the given type of process $\Delta E = \Delta E^c$ for condensation is opposite to $\Delta E = \Delta E^e$ for evaporation, the relationship

$$\frac{C^a}{E^a} = e^{\beta(\Delta\mu - \Delta E^c)} \tag{9}$$

holds.

It should be noted that the quantities C^a and E^a, as given by (8), are *not* probabilities for the acceptance of a Monte Carlo move (C^a may well be larger than 1). A large value of C or E means simply a short *time* before the corresponding move is made. The alternative choice, $\{\exp[\beta(\Delta E \mp \Delta\mu)] + 1\}^{-1}$, where the upper sign is for condensation and the lower one for evaporation, is more symmetric and elegant mathematically and corresponds better to the spirit of the Monte Carlo method, but the resulting rates of growth have no physical meaning. In the present formulation only the condensation rate (and not the evaporation rate) depends on $\Delta\mu$, i.e., on the vapor pressure, as it should. We prefer here physical significance to mathematical beauty.

The time evolution of the surface is given by the master equations for the probability $P(\{v\}, t)$ of the given configuration $\{v\}$ at time t

$$dP(\{v\}, t)/dt = -\sum_a \left(C^a p^a(\{v\}) + E^a q^a(\{v\})\right) P(\{v\}, t) + \sum_{a, \{\tilde{v}\}} \left(C^a M^a_{v\tilde{v}} + E^a N^a_{v\tilde{v}}\right) P(\{\tilde{v}\}, t) \tag{10}$$

where $p^a(\{v\})$, resp. $q^a(\{v\})$, is the number of condensation, resp. evaporation, sites for the given process (i.e., the number of the relevant plaquettes of vertices) in the configuration $\{v\}$ (we shall call them multiplicities), and $M^a_{v\tilde{v}}$, resp. $N^a_{v\tilde{v}}$, is the number of ways by which condensation, resp. evaporation, leads to a transition from the configuration $\{v\}$ to $\{\tilde{v}\}$ via the given process. The reciprocity relationship $N^a_{v\tilde{v}} = M^a_{\tilde{v}v}$ holds.

We study our kinetic six-vertex model on a finite size table $N \times N$ with periodic boundary conditions for the vertices. (This corresponds to

periodic boundary conditions for the level *differences* of neighboring atoms.) The number of possible configurations increases very rapidly with N. All configurations can be separated into classes invariant under the growth and evaporation processes (i.e., two configurations belong to the same class if they can be connected by a sequence of processes). We show that different classes correspond to surfaces with different Miller indices. Let us call n_α, resp. m_α, $\alpha = 1, 2, 3, 4, 5, 6$ the number of vertices of type α in the row, resp. column, of the $N \times N$ table. Let the rows be labeled from top to bottom. Then the sum $H = n_2 + n_3 + n_6$ for the nth row is the number of arrows between the $(n-1)$th and the nth row pointing down, i.e., in the line representation of the six-vertex model it is the number of lines crossing the nth row and due to line conservation[26] it is the same for all rows. Since the down arrows correspond to a decrease of the level of the surface atoms in the direction from left to right, the level difference between the left and the right edges of our table is $D_H = H - (N - H) = n_2 + n_3 - n_1 - n_4$, and it is the same for all rows. (Here we have used the fact that $n_5 = n_6$.) Analogously, the level difference between the bottom and the top is $D_V = m_1 + m_3 - m_2 - m_4$, and is the same for all columns. It is easy to check that the numbers D_H and D_V are conserved by all processes (2)–(7). On the other hand, two configurations with the same differences D_H and D_V belong to the same class. Hence, the class is characterized by a pair of numbers (D_H, D_V). Since each of them can take $N+1$ values $-N$, $-N+2, \ldots, N-2, N$ there are $(N+1)^2$ classes for given N.

Using the symmetry with respect to rotation by multiples of $\pi/2$ around the z axis and the reflection with respect to the (x, z) plane, the study can be restricted to the classes $D_V \geqslant 0$, $D_H \leqslant 0$, $|D_H| \leqslant D_V$. This corresponds to the restriction to surfaces with nonnegative Miller indices fulfilling $h \leqslant k$. After this restriction the number of classes is $C_N = \frac{1}{2}C(C+1)$, $C = [N/2] + 1$. C of them, for $D_V = N$, are passive, i.e., they do not allow any process to be realized in their configurations. The passive classes appear due to the restriction on the difference of the levels of n.n. sites in van Beijeren's model. The passive configurations contain only vertices 1 and 3 and correspond to the surfaces with monotonically increasing levels in some direction and Miller indices fulfilling $h + k = l$.

Taking into account the rotation by $\pi/4$ between our table and the axes of the bcc crystal, we find that the class (D_V, D_H) corresponds to the surface with the Miller indices (h, k, l) given by

$$h = (D_V - |D_H|)/u, \qquad k = (D_V + |D_H|)/u, \qquad l = 2N/u \tag{11}$$

where u is the largest common factor of $D_V - |D_H|$, $D_V + |D_H|$, and $2N$. For any given N we get a set of admissible surfaces. The hierarchy of these

surfaces for increasing N has the following property: If the surface with the Miller index (h, k, l) occurs for size N_o [class (D_V, D_H)], then it will appear for all sizes N multiple of N_o, $N = kN_o$ [class (kD_V, kD_H)]; k is any integer. In particular, class (0, 0) corresponds to the (0, 0, 1) surface for any even N.

An important quantity is the growth rate G. In general it depends on time: if the system at time t is in configuration $\{v\}_t$, the growth rate is

$$G(t) = \sum_a (C^a p^a(\{v\}_t) - E^a q^a(\{v\}_t)) \tag{12}$$

The mean growth rate is given by

$$\begin{aligned} \langle G \rangle &= \sum_a (C^a \langle p^a \rangle - E^a \langle q^a \rangle) \\ \langle p^a(t) \rangle &= \sum_{\{v\}} p^a(\{v\})\, P(\{v\}, t),\ \langle q^a(t) \rangle = \sum_{\{v\}} q^a(\{v\})\, P(\{v\}, t) \end{aligned} \tag{13}$$

where the averages in $\langle p^a \rangle$ and $\langle q^a \rangle$ are taken over the configurations in one class. When the system reaches the steady state, the average multiplicities $\langle p^a \rangle$ and $\langle q^a \rangle$ and also the mean rate of growth $\langle G \rangle$ become time-independent. Since $\langle G \rangle$ increases trivially with the number of sites N^2 in the table, in the following we shall study the rate of growth per site $G = \langle G \rangle / N^2$. To calculate G one has to solve two problems: (i) to find the distribution of the multiplicities $p^a(\{v\})$ and $q^a(\{v\})$ in a space of configurations; (ii) to solve the master equations for $P(\{v\})$. The exact solution of the six-vertex model is known[25,26]; it gives, however, only the free energy, whereas our multiplicities p^a, q^a are high-order, four-site correlation functions. Even if they were calculated, it is unlikely that the complicated master equations could be solved analytically. In this situation we turn to numerical solution for finite size N. Exact solutions of the master equations are found for very small N; for larger N, Monte Carlo simulations are performed. The former serve us mainly as a test of the latter.

3. EXACT FINITE-SIZE CALCULATION

The calculations can be simplified using the fact that the configurations differing only by translation (i.e., for periodic boundary conditions, by cyclic permutation of rows and/or columns) have the same time evolution. Then each class can be divided into subclasses S_m, where configurations in the same subclass differ only by translation, and instead of the probability $P(\{v\})$ it is sufficient to calculate a probability $P_m(t) = \sum_{\{v\} \in S_m} P(\{v\}, t)$ that the system at time t is in a configuration belonging

to the mth subclass. The time evolution within the class is described by the master equation

$$dP_m/dt = -\sum_a (C^a p_m^a + E^a q_m^a) P_m(t) + \sum_{a,n} (C^a M_{mn}^a + E^a N_{mn}^a) P_n(t) \tag{14}$$

where p_m^a and q_m^a are the multiplicities in the mth subclass. They are the same for all configurations in the subclass. M_{mn}^a (resp. N_{mn}^a) equals the number of ways p_{mn}^a (resp. q_{mn}^a) in which a condensation (resp. evaporation) process generates, from the configurations belonging to the subclass n, the configurations belonging to the subclass m, divided by the number N_n of configurations in the subclass n. Since the subclass n contains N_n equivalent configurations, then p_{mn}^a (resp. q_{mn}^a) is equal to N_n times the number of ways in which a condensation (resp. evaporation) process generates, from one given configuration in the subclass n, a configuration belonging to the subclass m. Further, since $p_{mn}^a = q_{nm}^a$, $N_{mn}^a = (N_m/N_n) M_{nm}^a$ holds.

The master equation (14) has some interesting properties. Let us first recall the well-known theorem[29,30] according to which all solutions of a master equation tend (under the appropriate hypotheses, that our master equation happens to satisfy) to one steady-state solution, irrespective of the initial conditions. This is equivalent to saying that, writing the master equation in the form

$$dP_m/dt = \sum_n L_{mn} P_n \tag{15}$$

all eigenvalues of $\mathbf{L}$ are negative, except for 0, which is nondegenerate.

In particular, van Kampen shows that certain quantities which he calls *entropies* are increasing functions of time (except of course in the steady state, where they stay constant).[30] There is considerable freedom in the choice of these quantities. The conventional choice, however, is $\sum_n P_n \ln(P_n^{\text{steady}}/P_n)$. For $\eta = 1$ [where $\eta = \exp(\beta \Delta\mu)$], i.e., at equilibrium, the latter reduces to

$$-F = -\sum_n P_n [E_n + kT \ln(P_n/N_n)] \tag{16}$$

(i.e., to minus the free energy, not to the entropy!). E_n is the energy of the configuration. For $\eta \neq 1$ no such simple form is available. However, we can prove the following (physically rather obvious, but comforting) result.

Theorem. In the steady state the mean growth rate $\bar{G}$ has the same sign as $\Delta\mu$.

The proof is simple. Let ω_n be the ratio P_n/P_n^{eq} between the probability of a subclass and the same at equilibrium. Then, by using the conventional method by which entropy is shown to increase (see e.g. van Kampen[31]) the time derivative of the free energy (16) is shown to be made up of two terms, of which the first is clearly nonpositive, being the sum of quantities of the form

$$(\eta\omega_m - \omega_n)\ln[\omega_n/(\eta\omega_m)] \tag{17}$$

multiplied by positive coefficients, and the second is

$$kTZ\bar{G}\ln\eta \tag{18}$$

(Z being the partition function). In the steady state the time derivative of F vanishes, and the theorem follows.

For low N it is relatively easy to classify all subclasses and to calculate the coefficients p_m^a, q_m^a, M_{mn}^a, N_{mn}^a. In the simplest case, $N=2$, there is only one active class $D_V = D_H = 0$, with six configurations, which separate into two subclasses. Only hill and lake processes take part in the transition between them. This is obviously insufficient to describe the nucleation. The solution of the equations (14) for the steady state gives the mean growth rate per site

$$G = \frac{e^{\beta\Delta\mu} - 1}{e^{4\beta\varepsilon} + 2e^{-4\beta\varepsilon} + 3} \tag{19}$$

i.e., the Wilson–Frenkel law[3] multiplied by a function of $\beta\varepsilon$ only.

Also in the case $N=3$ there is only one active class $D_V = 1$, $D_H = -1$. It has four subclasses and the exact solution can be easily obtained. Since the analytic expression is rather lengthy, we do not write it explicitly. The example of the dependence of G on the disequilibrium variable $\beta\mu$ for three temperatures is plotted in Fig. 4. The temperature is compared with the roughening temperature T_R of the six-vertex model $k_B T_R = \varepsilon/\ln 2$. Still not all processes are realized for $N=3$ (ridge and valley processes are missing), but all possibilities for the change of the number of bonds to the n.n.n. are allowed.

The number of subclasses for $N \geqslant 4$ increases so much that the problem cannot be solved analytically without the help of a computer. For example, for $N=4$ there are three nonequivalent active classes, of which the largest has 70, the second 23, and the third 10 subclasses.[32] However, even using the computer for the classification in subclasses and then for the

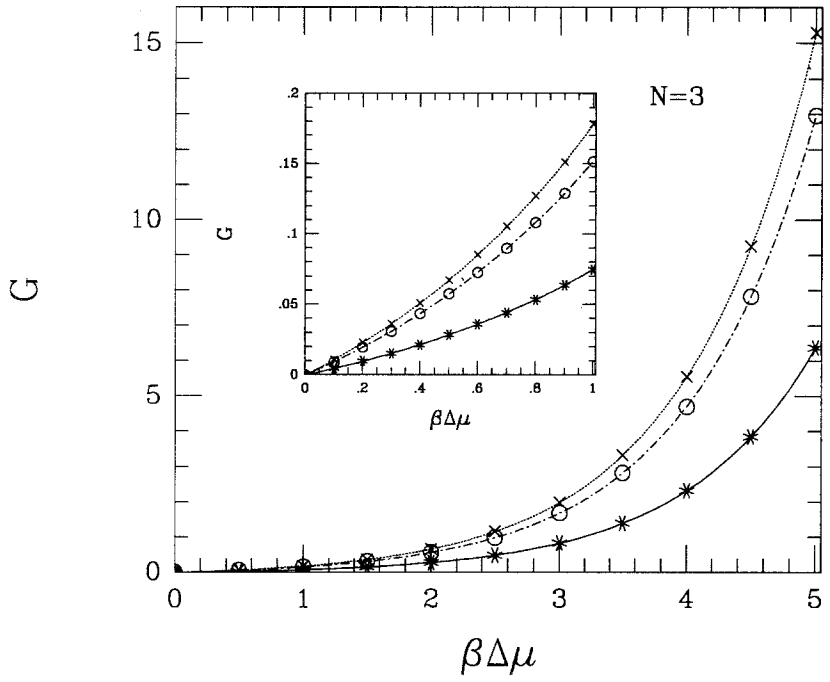

Fig. 4. The dependence of the growth rate per site G on disequilibrium $\beta\,\Delta\mu$ for $N=3$, active class, (013) surface. The curves correspond to the exact solution for different temperatures: $T/T_R=0.5$ (solid curve), $T/T_R=1$ (dashed-dotted curve), and $T/T_R=2$ (dotted curve). The points are results of the Monte Carlo simulation.

solution of the master equations, we are still limited to low N ($N=5$ or 6).[15] Although it may be pleasant to have exact results, such small sizes are clearly insufficient for the study of the nucleation phenomena, because to observe the latter the size of the system has to be much larger than the size of the critical cluster which (if such a cluster exists at all) increases, when $\beta\,\Delta\mu$ goes to zero, as $1/(\Delta\mu)^q$, $q\geqslant 1$.[3]

[3] This may be shown as follows. The free energy of a cluster is given by $F=-A\,\Delta\mu n+B\varepsilon n_b$, where n is the number of atoms in the cluster and n_b in its boundary. Let D be the dimensionality of the cluster and D' that of the boundary; then $n=\alpha L^D$, $n_b=\beta L^{D'}$, where L is a typical length. The critical cluster corresponds to the maximum free energy. Let us first assume D to be 2. Finding the maximum, the size L_c of the critical cluster is found to be proportional to $(\Delta\mu)^{-1/(2-D')}$; i.e., $q=(2-D')^{-1}$. If the boundary of the cluster is regular, $D'=1$, $q=1$. If, however, the boundary of the cluster is fractal, or more generally self-affine (which may happen whether the cluster is itself a fractal or not) $D'>1$; therefore $q>1$. If, on the other hand, $D<2$ (i.e., the cluster is a fractal), then $D'=D$ and there is no critical cluster.

Hence, the results of any finite-size calculation become incorrect in the nucleation regime (low temperature and low disequilibrium) for $\Delta\mu$ below some critical value $\Delta\mu_c$.

4. SIMULATION

For the more extensive studies of our model we have used a Monte Carlo simulation. It is founded on the ergodicity of the model. We start from some configuration and after a sufficient number of steps we obtain the quantities characteristic for the system. In each step of our simulation the processes possible in the given configuration together with their multiplicities are known. The probability of the condensation, resp. evaporation, process of the type a is $C^a p^a(\{v\})/Q(\{v\})$, resp. $E^a q^a(\{v\})/Q(\{v\})$, where $Q(\{v\}) = \sum_a (C^a p^a(\{v\}) + E^a q^a(\{v\}))$. One random number is used to decide which process will take place and a second random number is generated to select one of the possible sites. Then the configuration is changed and multiplicities are recalculated. To do that one needs only to look at the change of nine plaquettes, the plaquette of the process and eight plaquettes surrounding it.

An alternative procedure would be the following: select a site at random and check if any process is possible on it. If it is the case, then realize it or not with probability proportional to C^a in the case of condensation and to E^a in the case of evaporation; otherwise select a new site. The method chosen here is more complicated, but it avoids the unsuccessful attempts in which no process is possible on the chosen site. Hence, we need a lower number of iterations to get the results with the same accuracy.

The system is considered to stay in the state $\{v\}$ for a time inversely proportional to the total probability of all possible processes $Q(\{v\})$ per unit time. To obtain the mean growth rate the time average over K steps is calculated:

$$\langle G \rangle = t^{-1} \sum_{n=1}^{K} \sum_{a} (C^a p^a(\{v\}) - E^a q^a(\{v\}))/Q(\{v\}) \tag{20}$$

Here the total time t is given by

$$t = \sum_{n=1}^{K} 1/Q(\{v\}) \tag{21}$$

Due to the ergodicity this time average goes to the configurational average for a sufficiently long time t. The accuracy has been checked by comparison with the exact solution for $N = 2$ and 3 (Fig. 4). In both cases convergence (and agreement with the exact result up to three valid digits) is obtained

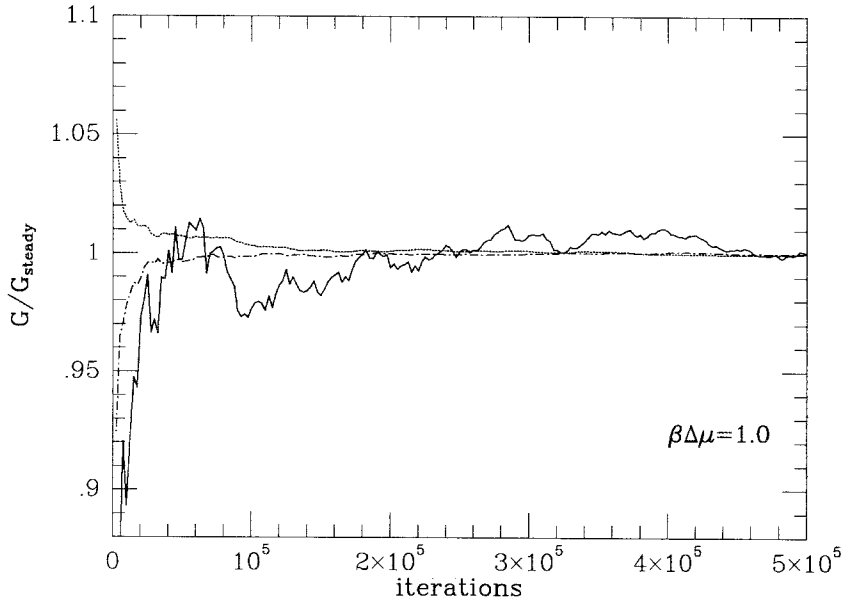

Fig. 5. The evolution of the calculated mean growth rate $\langle G \rangle$ during the simulation for $N = 32$, (001) surface, $\beta \Delta\mu = 1$, and three temperatures as in Fig. 4.

already after 10,000 steps. For large N the quantity $\langle G \rangle$, of course, oscillates much longer (see Fig. 5). For $T \geqslant T_R$, $\beta \Delta\mu \geqslant 1$, and the size up to $N = 32$ the convergence is obtained after 500,000 steps. The necessary number of iterations increases with decreasing temperature and chemical potential difference between vapor and crystal and for small disequilibrium or low temperature usually many more steps are needed. For $T = 0.5T_R$ and $\beta \Delta\mu \approx 1$ we need typically $2 \cdot 10^6$ steps.

Before studying the physics we have explored the finite-size effects. The dependence of the calculated growth rate per site for the (001) surface on N for the temperature $T = 0.5T_R$ and several values of the disequilibrium $\beta \Delta\mu$ is plotted in Fig. 6. For the higher temperatures the situation is better: the dependence is weaker. These results suggest that finite-size effects are small for $N \geqslant 32$. Hence, the majority of our calculations have been done for $N = 32$, and for the (001) surface.

5. RESULTS AND DISCUSSION

An example of the dependence of the growth rate per site G on disequilibrium for small and large values of $\beta \Delta\mu$ is given in Fig. 7. The data

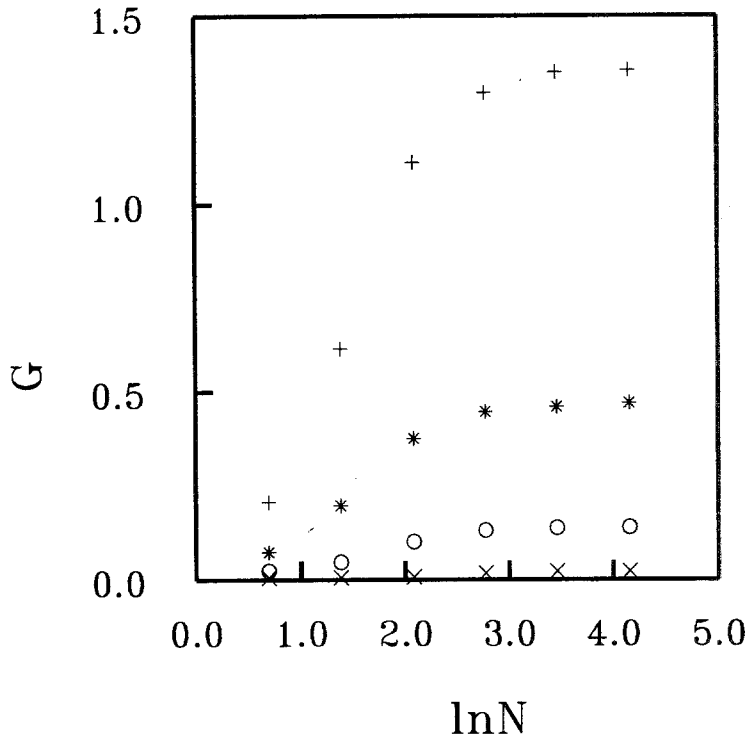

Fig. 6. The dependence of the growth rate per site G on size N of the table for (001) surface, $T/T_R = 0.5$, and several values of disequilibrium $\beta\,\Delta\mu = 1$ (crosses), $\beta\,\Delta\mu = 2$ (circles), $\beta\,\Delta\mu = 3$ (stars), $\beta\,\Delta\mu = 4$ (plus signs).

for six different temperatures are compared with the Wilson–Frenkel law $G \sim (e^{\beta\,\Delta\mu} - 1)$ in Fig. 8. We see that for large disequilibrium and large temperatures the agreement is quite good, whereas for the temperatures lower than or equal to T_R it breaks down in the low-disequilibrium region; for example, for $T = 0.5T_R$ it breaks down for $\beta\,\Delta\mu \leqslant 3$. From this plot we can also extract the temperature-dependent prefactor in the Wilson–Frenkel law. At high temperatures (above T_R) and small disequilibrium the Wilson–Frenkel predicts linear growth, i.e., G is proportional to $\beta\,\Delta\mu$. This is indeed the case in the present simulations. The limit

$$\tilde{K} = \lim_{\Delta\mu \to 0} \frac{G}{\beta\,\Delta\mu} \tag{22}$$

is shown in Table I. It behaves in a way somewhat similar to the coefficient K of the logarithm in the equilibrium mean square height difference,[33]

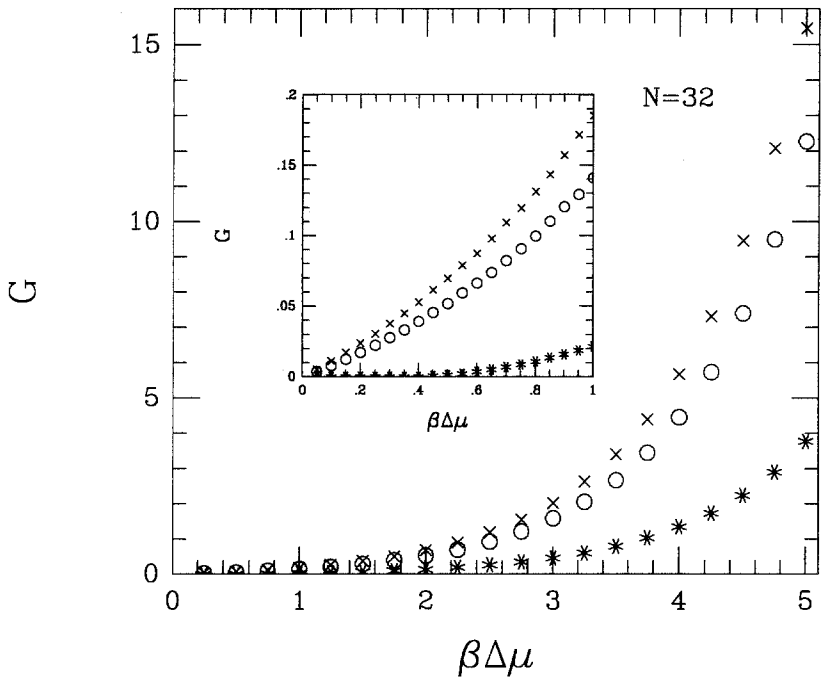

Fig. 7. The dependence of the growth rate G on the disequilibrium $\beta\,\Delta\mu$ calculated by the Monte Carlo simulation, for (001) surface, $N=32$, and for three different temperatures: $T/T_R=0.5$ (stars), $T/T_R=1$ (circles), and $T/T_R=2$ (crosses).

vanishing in the smooth phase (actually, due to finite-size effects, we find a nonvanishing $\tilde{K}$ just below T_R), increasing abruptly at T_R, and then slowly as $T\to\infty$ ($\tilde{K}$, however, saturates to the infinite-temperature limit faster than K).

It is expected that the nucleation phenomena will be important for low temperatures and disequilibria. We have compared the data for this range of parameters with the predicted Becker–Döring law for the rate of growth by nucleation as a function of $\Delta\mu$: $G\sim\exp(-\beta E^2/\Delta\mu)$.[21,3] Here E is a parameter with the dimensions of energy depending on the temperature and with only weak dependence on disequilibrium. (E is closely related to the step energy per unit length). In Fig. 9 we have plotted the quantity $\beta\,\Delta\mu\ln G$ (versus $\beta\,\Delta\mu$), which should be linear in $\beta\,\Delta\mu$ if the Becker–Döring law held with constant E. Only very roughly can one say that there is a region of $\beta\,\Delta\mu$ and T where this law is at least approximately fulfilled. However, our data are compatible with a law for the rate of growth by nucleation of the form $G\sim(\beta\,\Delta\mu)^r\exp(-\beta E^2/\Delta\mu)$.[3] The deviation from

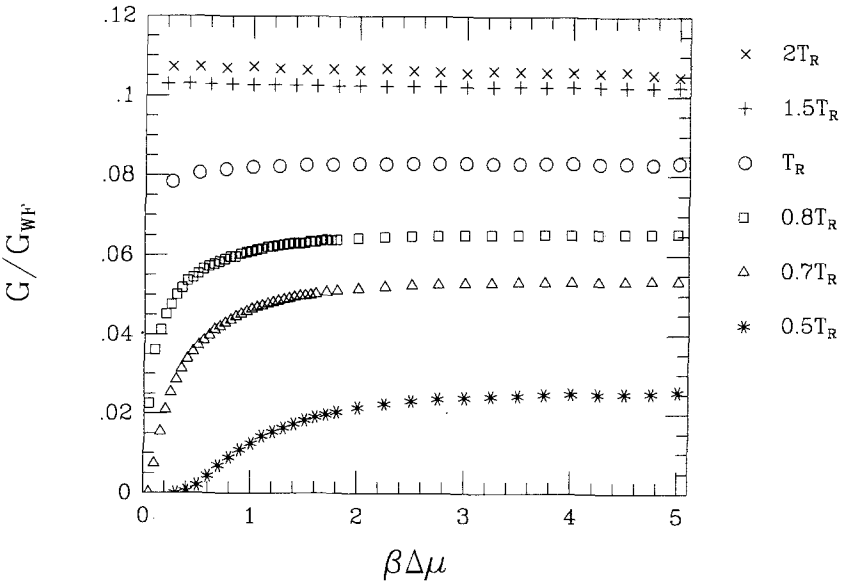

Fig. 8. The ratio of the calculated growth rate G to the Wilson–Frenkel law for several temperatures.

this law for very small $\beta\Delta\mu$ is a finite-size effect. Extrapolating this quasi-linear dependence on $\beta\Delta\mu$ to $\Delta\mu = 0$, we can obtain values of E. They decrease with increasing temperature in agreement with the expected vanishing of the step energy as $T \to T_R$.

The prefactor is the so-called "Zeldovich factor" and the recommended value for r in the literature is 5/6.[3,36] In the case of clusters with a fractal

Table I. Comparison between $\tilde{K} = \lim_{\Delta\mu \to 0} G/(\beta\,\Delta\mu)$ and the Coefficient K of the Logarithmic Asymptotic Behavior of the Half Mean Square Height Difference

T/T_R	$\tilde{K}$	$K/2$
0.8	0.000	0
0.9	0.020	0
1.0	0.070	$0 \to 0.051$
1.2	0.092	0.072
1.5	0.102	0.087
2.0	0.104	0.101
4.0	0.104	0.125

(or self-affine) boundary the disequilibrium $\Delta\mu$ in the exponential would be raised to the power q, $q>1$, but we find that in our case the growing clusters are always compact and, at least for layer-by-layer growth, have a regular boundary, i.e., $q=1$. Our present simulations are not accurate enough to estimate r, because with the given size $N=32$ we cannot perform the calculations for sufficiently small $\beta\Delta\mu$, as discussed above. For better understanding a more detailed description of the nucleation clusters is also needed. The work on this problem is in progress.

For medium $\beta\Delta\mu$ there is a crossover between nucleation and Wilson–Frenkel type behavior, corresponding to the transition between layer-by-layer (Frank–van der Merwe) ad continuous (Volmer–Weber) growth. This is seen in the change of the time evolution of the average height $\bar{h}$ for the given temperature with increasing $\beta\Delta\mu$ (Fig. 10). Here we have introduced a dimensionless variable $\Delta\tilde{\mu}=\Delta\mu/k_B T_R$.

To determine the ranges of parameters where these two different modes of growth apply, we change the variables from $(\beta\Delta\mu, T)$ to $(\Delta\tilde{\mu}, T)$ and employ the different temperature dependence of the growth rate according to the Becker–Döring law (increasing with temperature) and the Wilson–Frenkel law (decreasing with temperature, since the rapid saturation of $\tilde{K}$ with increasing temperature implies that the main temperature

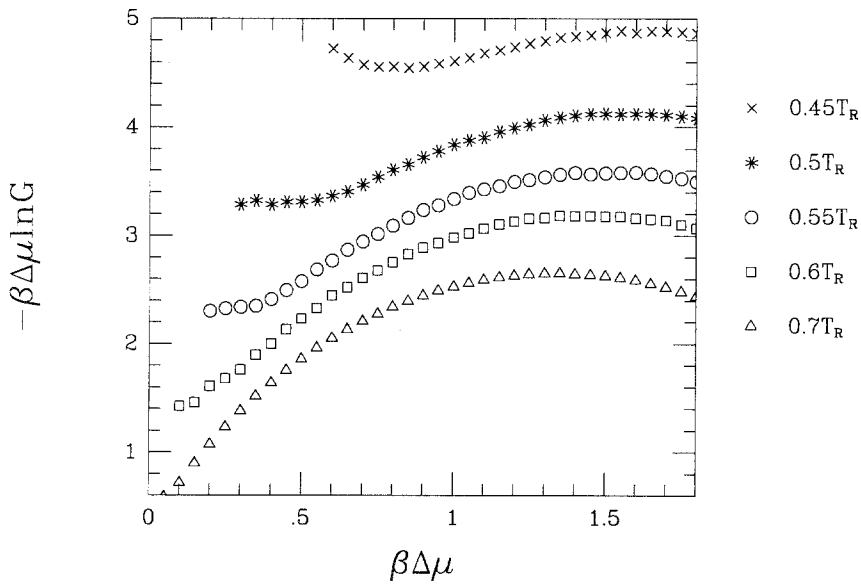

Fig. 9. The dependence of $-\beta\Delta\mu\ln G$ in the nucleation regime, as calculated by the Monte Carlo simulation, on $\beta\Delta\mu$ for $N=32$ and different temperatures.

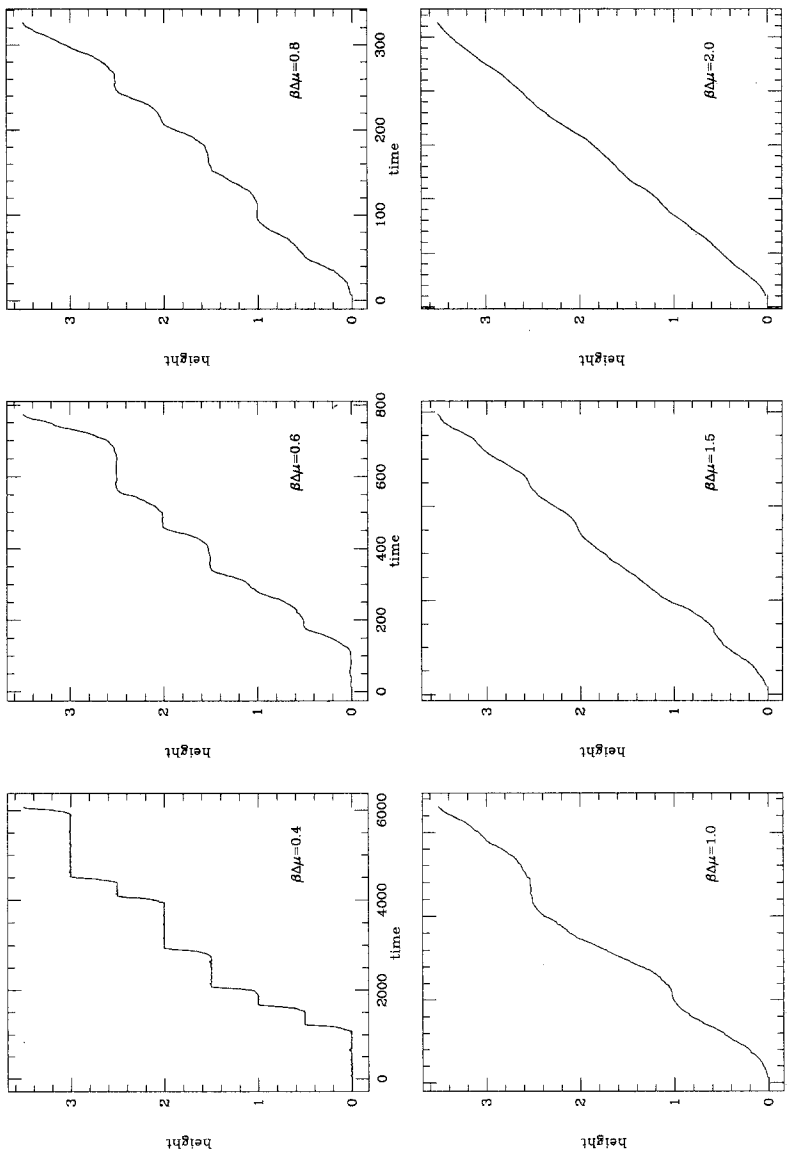

Fig. 10. The time dependence of the average height on (001) surface in units of the bcc spacing a for $T/T_R = 0.5$, $N = 32$, and several values of the disequilibrium.

dependence is due to the Wilson–Frenkel factor $e^{\beta \Delta\mu} - 1$). Then the curve in the $(\Delta\tilde{\mu}, T)$ plane separating the two modes can be approximately calculated by finding the temperature corresponding to the maximum growth rate for constant $\Delta\tilde{\mu}$. This needs very accurate calculation of the growth rate. The diagram obtained in this way is shown in Fig. 11. A similar diagram was obtained by Bennema and Gilmer[35] using a condition on the existence of minima in the Gibbs free energy.

The Becker–Döring-like form of the dependence of growth rate should disappear for large disequilibrium even at low temperatures because for $\Delta\tilde{\mu} > \Delta\tilde{\mu}_{at}$ already one adatom is the critical cluster. Indeed, the separating curve for very low temperatures and large disequilibrium goes up and then it suddenly turns to the $T = 0$ axis. There is a critical value $\Delta\tilde{\mu}_c$ such that for $\Delta\tilde{\mu} > \Delta\tilde{\mu}_c$ there is no maximum in the growth rate for constant $\Delta\tilde{\mu}$ (although at low temperature there is still layer-by-layer growth in the case

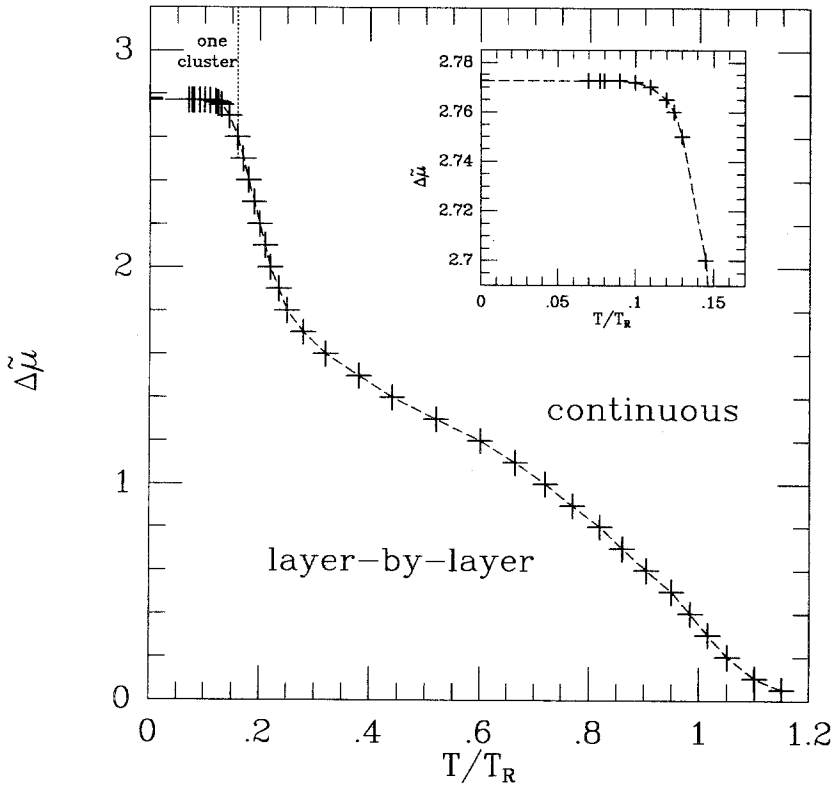

Fig. 11. The regions of different modes of growth in the $(\Delta\tilde{\mu}, T)$ plane. The dotted line indicates the region of the one-cluster mode of growth.

of the finite system, see below). For $N=32$, $\Delta\tilde{\mu}_c = 2.773$ and this value is only weakly dependent on the size.

A direct check of the configurations confirmed that sufficiently inside the region of continuous growth the crystal really grows by the formation and expansion of many small clusters, not only in one layer, but also one on the other, with a surface width of several layers, whereas in the layer-by-layer region the growth is due to the expansion of a few large clusters in one or two layers. We have, however, found that for small temperature and large disequilibrium up to $\Delta\tilde{\mu}=5$ the crystal still grows in the layer-by-layer mode, mostly with one expanding cluster, i.e., with one growing layer only. This can be explained by a comparison of the probability P_{exp} that in the configuration with one cluster the cluster will expand with the probability P_{adat} that another adatom will be added by the hill process. This, of course, depends on the size N of the table. For sufficiently large N, $P_{\text{exp}} < P_{\text{adat}}$ holds; but for a given size there exists a critical temperature

$$T^*(N) \approx T_R \frac{\ln 2}{\ln(N/2\sqrt{2})}$$

below which $P_{\text{exp}} > P_{\text{adat}}$ independently of $\Delta\tilde{\mu}$ [$T^*(32) \approx T_R/3$]. On the other hand, for sufficiently large $\Delta\tilde{\mu} > \Delta\tilde{\mu}^*$ the probability P_{exp} that the cluster will grow is also larger than the probability P_{evap} that it will evaporate, even for one adatom. $\Delta\tilde{\mu}^*$ depends on the temperature; for low temperature, $\Delta\tilde{\mu}^* \approx 2 \ln 2 \doteq 1.39$. Hence the growth takes place by a one-cluster mode. Since $T^*(N)$ is a decreasing function of N, however, this one-cluster mode is a finite-size effect and we do not expect it to be present for an infinite system. We believe that the separating curve for the infinite system crosses the $T=0$ axis.

At the opposite end the correct separating curve should go through the point ($T=T_R$, $\Delta\tilde{\mu}=0$) because for $\Delta\tilde{\mu}=0$ and $T>T_R$ the surface is always rough (and the disequilibrium can only destroy the smoothness of the surface). Our line goes to higher temperatures as $\Delta\tilde{\mu}\to 0$. This is due to the approximative way in which it was determined, which can only reflect its qualitative features. Our data suggest that the line is turning to the right as $\Delta\tilde{\mu}\to 0$. This is consistent with the result of the dynamic roughening theory[36] that it should meet the temperature axis tangentially. (The exact form of this dependence is, of course, difficult to verify numerically.)

One can expect that the two modes of growth may also differ in the dependence of the mean square height difference $w^2 = (1/N^2) \sum_i \langle (h_i - \bar{h})^2 \rangle$, [where $\bar{h} = (1/N^2) \sum_i h_i$], on the size N. For both growth

modes w appears to diverge with increasing N, probably according to different laws, the roughness being of course milder (logarithmic?) in the layer-by-layer mode and stronger in the continuous mode. However, whether a sharp kinetic roughening transition really exists in our model and the nature of its connection with transition between growth modes remain to be investigated. Work on this problem is in progress.

In this paper we have concentrated on the study of the growth on the (001) surface. A further interesting problem under investigation concerns the dependence of the rate of growth on the Miller indices of the surface.

ACKNOWLEDGMENT

It is a pleasure for the authors to gratefully acknowledge fruitful discussions with M. Touzani. The classification of subclasses within the various classes for size 4 is due to him.

REFERENCES

1. W. K. Burton, N. Cabrera, and F. C. Frank, *Phil. Trans. R. Soc. A* **243**:229 (1951).
2. J. D. Weeks, in *Ordering in Strongly Fluctuating Condensed Matter Systems*, T. Riste, ed. (Plenum Press, New York, 1980); H. van Beijeren and I. Nolden, in *Structure and Dynamics of Surfaces II*, W. Schommers and P. von Blackenhagen, eds. (Springer-Verlag, Berlin, 1987); I. Nolden, Thesis, University of Utrecht (1990).
3. J. D. Weeks and G. H. Gilmer, *Adv. Chem. Phys.* **40**:157 (1979).
4. F. Family and T. Vicsek, *J. Phys. A* **18**:L75 (1985).
5. M. Kardar, G. Parisi, and Y. C. Zhang, *Phys. Rev. Lett.* **56**:889 (1986).
6. S. T. Chui and J. D. Weeks, *Phys. Rev. Lett.* **40**:733 (1978).
7. P. Nozières and F. Gallet, *J. Phys.* **48**:353 (1987).
8. T. Hwa, M. Kardar, and M. Paczuski, preprint.
9. J. Kertész and D. E. Wolf, *Phys. Rev. Lett.* **62**:2571 (1989); C. Lehner, N. Rajewsky, D. E. Wolf, and J. Kertész, *Physica A* **164**:81 (1990); J. Krug, J. Kertész, and D. E. Wolf, *Europhys. Lett.* **12**:113.
10. J. G. Amar and F. Family, *Phys. Rev. Lett.* **64**:1405 (1990).
11. H. Yan, D. Kessler, and L. M. Sander, *Phys. Rev. Lett.* **64**:926 (1990).
12. H. Guo, B. Grossmann, and M. Grant, *Phys. Rev. Lett.* **64**:1262 (1990).
13. B. M. Forrest and L.-H. Tang, *Phys. Rev. Lett.* **64**:1405 (1990).
14. Y. P. Pellegrini and R. Jullien, *Phys. Rev. Lett.* **64**:1745 (1990).
15. C. Garrod, A. C. Levi, and M. Touzani, *Solid State Commun.* **75**:375 (1990).
16. F. Y. Wu, *Phys. Rev.* **168**:539 (1968).
17. C. Garrod, *J. Stat. Phys.* **63**:987 (1991).
18. B. M. Forrest and L.-H. Tang, *J. Stat. Phys.* **60**:181 (1990).
19. D. J. Gates and M. Westcott, *Proc. R. Soc. Lond. A* **40**:443 (1988); **40**:463 (1988); D. J. Gates, *J. Stat. Phys.* **52**:259 (1988).
20. C. Garrod, *Phys. Rev. A* **41**:4184 (1990).
21. R. Becker and W. Döring, *Ann. Phys. (Leipzig)* **24**:719 (1935).
22. M. den Nijs, *Phys. Rev. Lett.* **64**:434 (1990).

23. H. van Beijeren, *Phys. Rev. Lett.* **38**:993 (1977).
24. L. Pauling, *J. Am. Chem. Soc.* **57**:2680 (1935); J. C. Slater, *J. Chem. Phys.* **9**:16 (1941).
25. E. H. Lieb and F. Y. Wu, in *Phase Transitions and Critical Phenomena*, Vol. 1, C. Domb and M. S. Green, eds. (Academic Press, London, 1972).
26. R. J. Baxter, *Exactly Solvable Models in Statistical Physics* (Academic Press, London, 1982).
27. P. Meakin, P. Ramanlal, L. M. Sander, and R. C. Ball, *Phys. Rev. A* **34**:5091 (1986).
28. R. J. Glauber, *J. Math. Phys.* **4**:294 (1963).
29. R. Cox and H. D. Miller, *The Theory of Stochastic Processes* (Methuen, London, 1965).
30. N. G. van Kampen, *Stochastic Processes in Physics and Chemistry* (North-Holland, Amsterdam, 1981).
31. N. G. van Kampen, in *Fundamental Problems in Statistical Mechanics I*, E. G. D. Cohen, ed. (North-Holland, Amsterdam, 1962).
32. M. Touzani, Private communication.
33. R. W. Youngblood, J. D. Axe, and B. M. McCoy, *Phys. Rev. B* **21**:5212 (1980).
34. A. A. Chernov, *Contemp. Phys.* **30**:251 (1989).
35. P. Bennema and G. H. Gilmer, in *Crystal Growth, An Introduction*, P. Hartman, ed. (North-Holland, Amsterdam, 1973).
36. S. Balibar, F. Gallet, and E. Rolley, *J. Crystal Growth* **99**:46 (1990), and references quoted therein.